Stronger Tropical Cyclone–Induced Ocean Cooling in Near-Coastal Regions Compared to the Open Ocean

NGUYEN DAC DA,[a,b] GREGORY R. FOLTZ,[c] KARTHIK BALAGURU,[d] AND ELEDA FERNALD[d,e]

[a] *Faculty of Meteorology, Hydrology and Oceanography, University of Science, Vietnam National University, Hanoi, Vietnam*
[b] *ISCALE Computing Solutions JSC, Hanoi, Vietnam*
[c] *National Oceanic and Atmospheric Administration/Atlantic Oceanographic and Meteorological Laboratory, Miami, Florida*
[d] *Pacific Northwest National Laboratory, Richland, Washington*
[e] *Watson Foundation, New York, New York*

(Manuscript received 15 November 2022, in final form 29 May 2023, accepted 1 June 2023)

ABSTRACT: Tropical cyclones (TC) often induce strong mixing in the upper ocean that generates a trail of cooler sea surface temperature (Twake) in their wakes. The Twake can affect TC intensity, so its prediction is important, especially in coastal regions where TCs can make landfall. Coastal Twakes are often more complex than those in the open ocean due to the influences of coastline geometry, highly variable water depth, continental runoff, and shelf processes. Using observational data since 2002, here we show a significantly stronger global mean Twake in coastal regions compared to offshore regions. Temperature stratification is the main driver of stronger coastal Twakes in the North Atlantic and east Pacific. In the northwest Pacific and north Indian Ocean, the differences between coastal and offshore Twakes are smaller due to compensation between TC forcings and ocean stratification. The north Indian Ocean is unique in the Northern Hemisphere because salinity stratification plays a major role on the spatial distribution of Twake. In the South Pacific Ocean, TC intensity and translation speed are crucial for explaining coastal–offshore Twake differences, while ocean stratification and mixed layer depth are more important for the coastal–offshore Twake differences in the south Indian Ocean. These findings suggest that coastal–offshore differences in ocean stratification need to be properly represented in models in order to capture changes in TC-induced ocean cooling as storms approach landfall.

SIGNIFICANCE STATEMENT: Landfalling tropical cyclones (TCs) often cause considerable damage in coastal regions with dense human populations. Understanding TC–ocean interaction and how it differs between coastal and offshore regions can help predict TC intensity prior to landfall. Sea surface cooling after TC passage is an important proxy for TC–ocean interaction. A global evaluation of coastal TC-induced cooling has not been conducted. Using data covering two decades, we show significantly stronger TC-induced surface cooling in coastal regions compared to offshore regions at the global scale and in all basins except the northwest Pacific and north Indian Ocean. The difference is driven mainly by upper-ocean conditions in the North Atlantic, east Pacific, and south Indian Ocean, and by TC characteristics in the South Pacific.

KEYWORDS: Oceanic mixed layer; Stability; Tropical cyclones; Air-sea interaction; Climate classification/regimes; Sea surface temperature

1. Introduction

Tropical cyclones (TCs) can inflict extensive damages in coastal regions, especially those that are densely populated (Pielke et al. 2008). Timely and accurate forecasts of TC tracks and intensities are therefore crucial for reducing their potential damage. Previous studies have shown that while the forecasting skill of TC tracks has improved significantly over the past several decades, TC intensity prediction has seen less overall progress and remains challenging, especially for storms that rapidly intensify (Kaplan et al. 2010; Cangialosi et al. 2020). Predicting TC intensity in coastal regions is more complicated because of the presence of coastlines, ocean bathymetry, coastal ocean dynamics, and continental freshwater runoff (Shen and Ginis 2003; Mahapatra et al. 2007; Glenn et al. 2016; Guan et al. 2021). Further, from an operational standpoint, accurate forecasts of TC intensity in coastal regions hold higher significance.

One of the most important predictors of TC intensity is sea surface temperature (SST), which affects the enthalpy flux between the ocean and atmosphere and largely determines the maximum potential intensity a TC can reach (Price 1981; Cione and Uhlhorn 2003; Emanuel 2003; Vincent et al. 2012). Under strong TC wind forcing, cooler subsurface water can be mixed and entrained into the surface layer, decreasing SST and the surface enthalpy flux, causing the TC to weaken (Cione and Uhlhorn 2003; Lin et al. 2003; Zhu and Zhang 2006). The magnitude of cooling depends on the TC's intensity, translation

Denotes content that is immediately available upon publication as open access.

Supplemental information related to this paper is available at the Journals Online website: https://doi.org/10.1175/JCLI-D-22-0842.s1.

Corresponding author: Nguyen Dac Da, nguyendacda@gmail.com

DOI: 10.1175/JCLI-D-22-0842.1

speed, size, ocean stratification, and mixed layer depth (Price 1981; Bender et al. 1993; Vincent et al. 2012; Balaguru et al. 2015; Zhang et al. 2019; Da et al. 2021; Wang and Toumi 2021): stronger TCs, slower TC translation, larger TCs, stronger ocean temperature stratification, weaker salinity stratification, and a thinner mixed layer are more favorable for stronger understorm cooling and larger SST wakes.

Coastal regions are often influenced by continental freshwater runoff, shallow bathymetry that limits the depth of the mixed layer, and coastline-influenced ocean dynamics. All of these factors may result in different magnitudes of TC-induced SST cooling compared to the open ocean. In offshore regions, turbulent mixing in the upper ocean can cause up to 85% of the surface cooling, with the remainder due to surface heat fluxes and Ekman upwelling (Price 1981). In contrast, in some shallow coastal regions, TC-induced surface heat fluxes can dominate the cooling (Shen and Ginis 2003). In offshore regions, the strongest TC-induced cooling usually occurs to the right of TC tracks in the Northern Hemisphere (Price 1981), whereas in coastal regions it can sometimes occur to the left owing to the influence of coastlines (Mahapatra et al. 2007). While the combination of strong stratification and coastal dynamics can result in much stronger ahead-of-eye cooling in some coastal regions (Glenn et al. 2016; Seroka et al. 2016; Guan et al. 2021), cooling can be reduced in some other regions when downwelling is prominent (Gramer et al. 2022). These processes need to be resolved in numerical weather forecast models for accurate TC intensity prediction at landfall. However, previous findings have been based mostly on case studies, and it is unknown if there are significant differences in TC-induced SST cooling between coastal and offshore regions at the global scale. In this study, we compare TC-induced cooling in coastal and offshore regions and assess the impacts of TC characteristics (intensity, translation speed, and size) and pre-TC ocean conditions (temperature and salinity stratification and mixed layer depth) on the differences.

2. Data and methods

a. Data

For storm-track data, we use the International Best Track Archive for Climate Stewardship (IBTrACS) dataset (version 4; Knapp et al. 2018). This dataset is a merged version of storm-track data from TC monitoring and warning centers around the world. We use TC positions, distance to land, and the World Meteorological Organization maximum sustained wind speeds (wmo_wind in the data file). To take into account the impacts of TC size on the coastal–offshore TC-induced cold wake (Twake hereafter for short) difference, we use the radius of 34-kt wind (1 kt $\approx$ 0.51 m s^{-1}) provided by U.S. institutions (usa_r34, R34 hereafter for short) with global coverage since 2002. R34 was chosen mainly because it has a larger sample size than R50 and R64 and is more correlated with predicted Twake based on dynamic temperature [see section 2d(2) for more details]. Our study period starts in 2002, when TC size data are first available, and extends to 2020.

For the computation of Twake, we use the microwave (MW; version 5.0) satellite SST dataset produced by Remote Sensing Systems (www.remss.com). This daily dataset is less affected by clouds and is available from 1998 onward. For intervalidation, we use the Optimum Interpolation Sea Surface Temperature (OISST) dataset version 2.1 created by the National Centers for Environmental Information (https://www.ncei.noaa.gov/). The data come with 0.25° and daily resolutions and cover the period from September 1981 to present. OISST combines SST data from in situ and infrared satellites, so its quality is impacted when there are clouds. The two SST datasets have similar cold wake variability over their common period (Da et al. 2021).

The role of ocean stratification in TC-induced SST cooling is assessed using temperature and salinity from the Simple Ocean Data Assimilation (SODA) reanalysis dataset version 3.4.2 (Carton et al. 2018), distributed by the University of Maryland (https://dsrs.atmos.umd.edu/). This dataset covers the study period 1982–2020 and is available at 5-day and ~0.5° resolution.

b. Twake and stratification index computation

1) Spatial and time average

In this study, we adopt the method for computing Twake and stratification indexes described in Da et al. (2021). For each TC time–location, Twake is the difference between area-averaged SST (over a 4° × 4° region centered at each TC's location) for the post-TC (averaged 1–3 days after) and pre-TC (averaged 2–4 days before) periods. The sensitivity of the coastal–offshore Twake difference to bin size will also be tested. For ocean stratification, we compute the pre-TC mean vertical temperature gradient (Grad-T) and salinity gradient (Grad-S) in the upper 100 m, averaged in a 4° × 4° region centered at each TC's location. The 100-m depth was found to be relevant for TC studies (Balaguru et al. 2015; Da et al. 2020). The gradients are the vertical slope of linear fits of temperature and salinity data from the surface to 100 m.

2) Mean and confidence intervals

The means and confidence intervals of Twake, TC characteristics, and ocean stratification are computed using a bootstrap method (Efron 1992), which gives estimates of the population mean and associated confidence intervals without any assumptions about the distribution of data. We randomly subsample with replacement 1000 times from the original data, using the same sample size as the original data. We then compute the mean of each of the 1000 samples and use the median (50th percentile) value of the 1000 samples of mean values as the final mean value. The confidence interval of the final mean is calculated as the 2.5–97.5 percentile interval of the 1000 values of the sample mean. Two mean values (e.g., coastal versus offshore) are considered significantly different if their confidence intervals do not overlap. We use Pearson correlation throughout this study, and the associated significance of a correlation is based on the p value. A correlation is considered to be significantly different than zero when the p value is lower than 0.05.

c. Coastal region definition

It is difficult to define the exact boundary that separates coastal and offshore regions because the effects of the coast and coastal ocean dynamics vary in time and space. For simplicity, we define

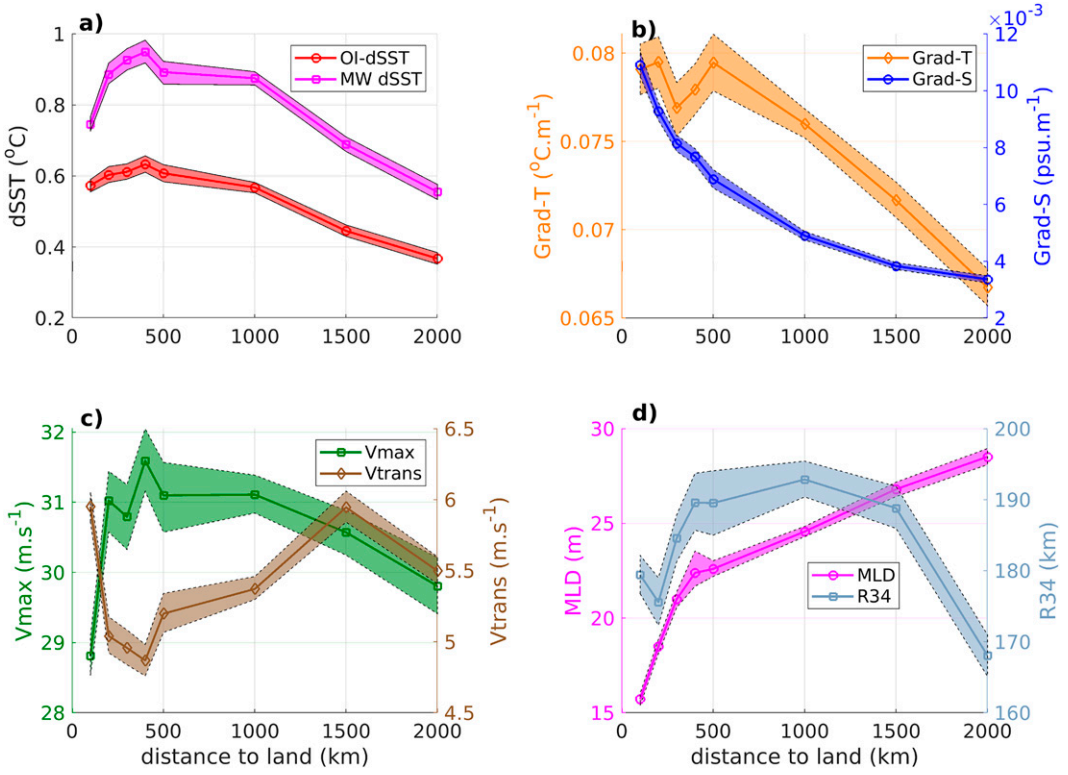

FIG. 1. Variation with respect to distance to land of (a) MW and OI Twake, (b) temperature and salinity stratification, (c) TC intensity and translation speed, and (d) TC radius of 34-kt wind and mixed layer depth. Shading represents 95% confidence intervals.

a boundary that in the context of TCs best preserves the distinct characteristics of coastal waters compared to offshore regions. Figure 1 shows the variations of global mean Twake, pre-TC ocean stratification, and TC characteristics as a function of distance to land. In offshore regions, Twake results from TC–ocean interactions. However, in coastal regions it may also be influenced by a TC's interaction with land, which generally reduces its intensity. Figure 1a shows that global mean Twake increases from the coast to about 400 km offshore, then decreases farther offshore. This behavior is observed in both OI and MW SST datasets.

The impacts of continental runoff and ocean circulation induced by coastlines and shallow bathymetry can result in very different ocean stratification and mixed layer depth (MLD) in nearshore and offshore regions. Figures 1b and 1d show the variations of Grad-T, Grad-S, and MLD with respect to distance from land. Grad-T remains relatively constant from the coast to 500 km offshore and then begins to decrease. In contrast, pre-TC mean Grad-S rapidly decreases from the coast to 500 km and then decreases at a slower rate farther offshore. MLD, however, rapidly increases from the coast to 400–500 km and then increases linearly farther offshore at a slower rate. Hence, if we base the near-coastal definition on pre-TC ocean stratification and MLD, ~500 km is a reasonable boundary.

Figures 1c and 1d show the variability of global mean TC intensity (Vmax), translation speed (Vtrans), and R34 with respect to distance from land. From 500 to 1500 km from the coast, Vmax gradually decreases and Vtrans gradually increases, while R34 shows little variation. Within 500 km of the coast, Vmax, Vtrans, and R34 show stronger variations. From 200 to 500 km of the coast, R34 significantly increases, while Vmax and Vtrans show little change in magnitude. However, from 200 km offshore to the coast, while R34 slightly increases, Vmax decreases rapidly, likely due to land friction effects, and Vtrans increases significantly. Thus, if we use TC characteristics to separate coastal and offshore regions, 400–500 km from the coast is a reasonable choice.

For simplicity, based on the different coastal/open-ocean regimes of Twake, stratification, and TC characteristics, we define the near-coastal region to be within 500 km of land. The resulting coastal and offshore TC locations are presented in Fig. 2. We performed a similar analysis with respect to water depth instead of distance to coast (see Fig. S1 in the online supporting document). It is noisier in general and more difficult to distinguish the coastal and offshore regions.

d. *Sensitivity analysis*

Coastal–offshore Twake differences may be caused by differences in TC characteristics (intensity, translation speed, size), pre-TC ocean conditions (Grad-T, Grad-S, MLD), or both. To assess the importance of each, we use two different approaches: a statistical analysis using a subsampling method and a theoretical approach using the dynamic temperature framework (Balaguru et al. 2015). We also looked at the meridional dependence of coastal–offshore Twake difference and did not find a strong contribution because coastal–offshore

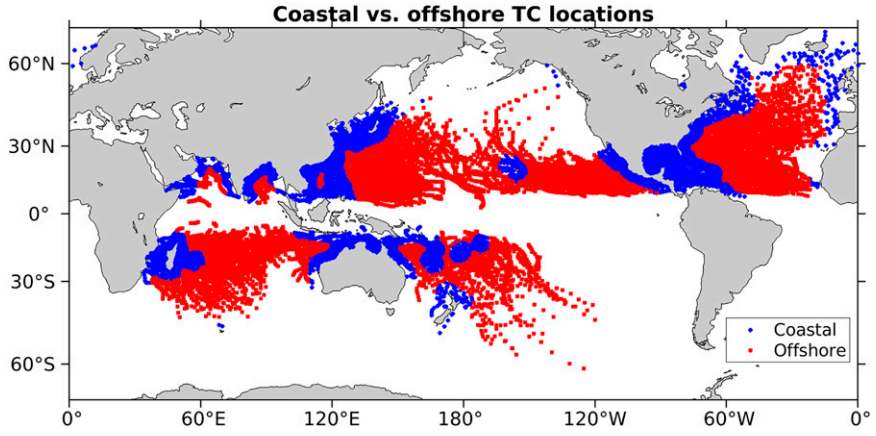

FIG. 2. Coastal vs offshore TCs locations.

regions are mainly separated zonally, not meridionally. Therefore, we do not include latitude in the analysis.

1) SUBSAMPLING TECHNIQUE

One way to separate the impacts of ocean conditions and TC characteristics on coastal–offshore differences in Twake is to subsample into two groups (coastal and offshore) that have the same TC characteristics (i.e., the same probability distributions and mean values of Vmax, Vtrans, and R34). The differences, if any, in the resulting mean value of Twake can then be attributed to pre-TC ocean conditions. The goal is to create two subsets, say A′ for coastal and B′ for offshore, that have similar distributions and are representative of the original data (A, B). Hence, for given subranges of Vmax, Vtrans, and R34, there should be the same amount of data in A′ and B′. We therefore divide the varying range of Vmax (15–105 m s^{-1}), Vtrans (0–20 m s^{-1}), and R34 (0–500 km) into smaller bins with sizes of 10 m s^{-1} for Vmax, 1 m s^{-1} for Vtrans, and 50 km for R34. Then we repeatedly consider all possible Vmax–Vtrans–R34 bin combinations. For each bin combination, we find all coastal and offshore values of Vmax, Vtrans, and R34 in A and B that fit the bin combination. The number of data falling in the bin combination from A and B can be different. Therefore, we keep the minimum number of data so that the two subsets A′ and B′ have similar distributions compared to A and B, respectively.

Table S1 in the supporting document shows the amount of data before and after subsampling for coastal and offshore regions in each basin and globally. The remaining percentage of data after subsampling is greater than 75% of the total data points in the coastal/offshore region with the least amount of data, except in the South Pacific (64%). Therefore, the ranges of values and sample sizes of the subsampled data are representative of the original data. Figure 3 shows the global distribution of Vmax, Vtrans, and R34 in coastal and offshore regions before and after subsampling. Before subsampling, the distributions of Vmax, Vtrans, and R34 between coastal and offshore regions do not pass the two-sample Kolmogorov–Smirnov test. After subsampling, the distributions pass the test and look similar, and the sample sizes are the same.

2) DYNAMIC TEMPERATURE ANALYSIS

To test the importance of different factors for driving Twakes in coastal and offshore regions, we use dynamic temperature (Tdy), which formulates the impacts of TC intensity, translation speed, and pre-TC ocean conditions on SST (Balaguru et al. 2015). First, a theoretical ocean mixing length induced by the TC is computed as

$$L = h + \left(\frac{2\rho_0 u_*^3 t}{\kappa g \alpha}\right)^{1/3}, \tag{1}$$

where h is the initial mixed layer depth, ρ_0 is seawater density, u_* is friction velocity, which is proportional to TC Vmax, $t = 2 \times R/$Vtrans is the time period of mixing, with R representing TC size and Vtrans the TC translation speed, κ is the von Kármán constant, g is the acceleration due to gravity, and α is density stratification beneath the mixed layer. Note that in the original formula of Balaguru et al. (2015), R is set to a constant of 50 km. In this study we use a variable TC size that represents the characteristic size of R64 (radius of 64-kt winds) and the variability of R34, which is empirically derived as $R' = 0.2848 \times \text{R34} - 1.7666$. More details on this empirical relationship can be found in text S1 of the supporting document.

Tdy, which represents SST under the core of the storm, is then calculated as

$$\text{Tdy} = \frac{1}{L}\int_{-L}^{0} T(z)dz, \tag{2}$$

where $T(z)$ is the pre-TC temperature profile. Twake is then deduced as

$$\text{Twake} = T(0) - \text{Tdy}, \tag{3}$$

where $T(0)$ is the pre-TC SST. Using Tdy, theoretical TC-induced wakes over the study period (2002–20) can be simulated using TC intensity, translation speed, and size from the IBTrACS dataset and pre-TC ocean temperature and salinity profiles from SODA. We label this the control analysis (CTRL). Figure 4

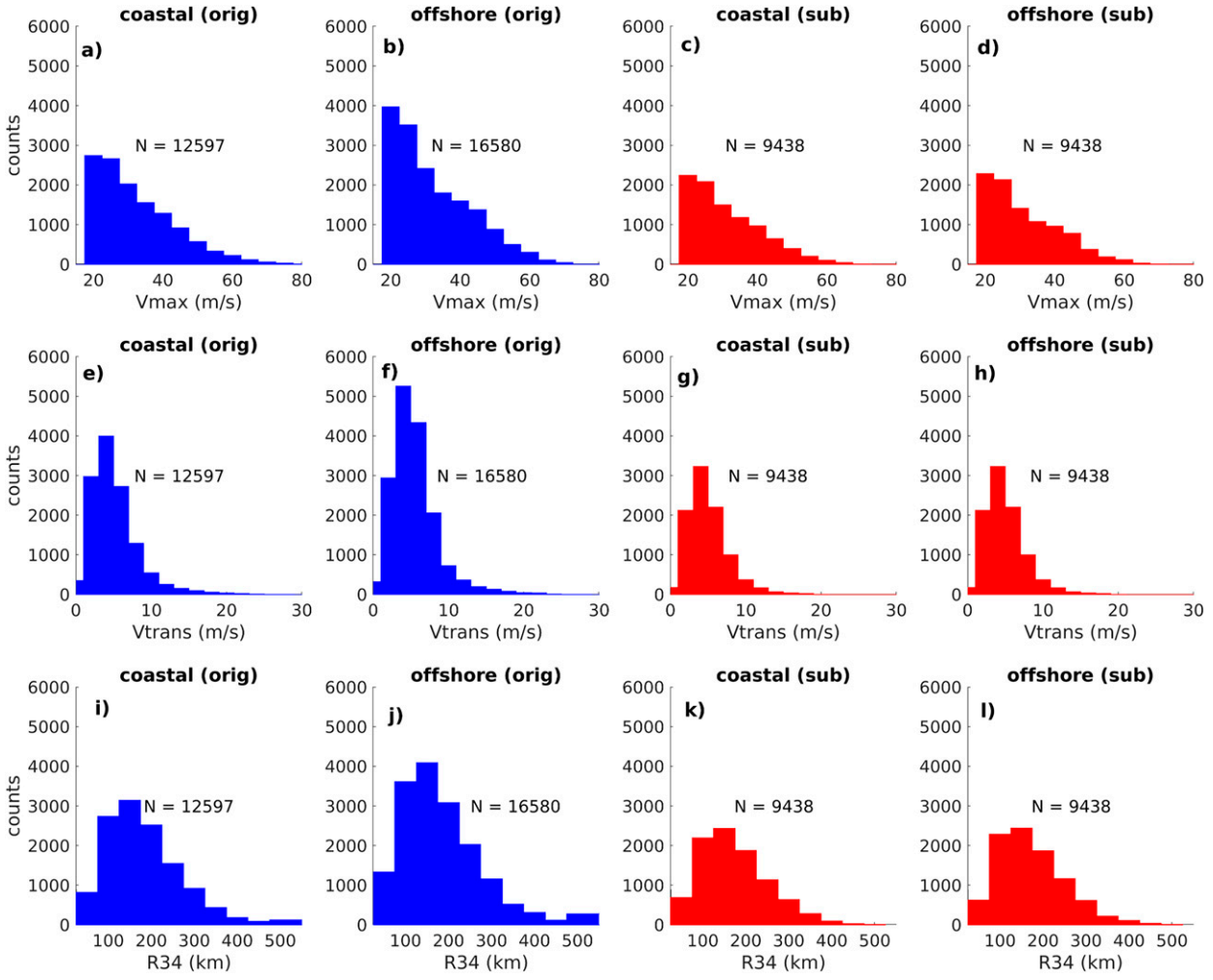

FIG. 3. Distributions of original (orig) and subsampled (sub) global TC intensity (Vmax), TC translation speed (Vtrans), and TC radius of 34-kt wind (R34) over the 2002–20 period. Here, *N* represents the total sample size in each plot.

compares CTRL Twake with MW Twake (Fig. 4b), using the relationship between OI and MW Twake as a reference (Fig. 4a). The correlation between OI and MW Twakes is 0.73 over their common period, with a bias of 0.26°C and residual standard error (RSE) of 0.58°C. This means that OI Twake can explain about 55% of the variance in MW Twake. However, OI Twake underestimates the mean magnitude of MW Twake (bias of 0.26°C). This is likely due to the impacts of clouds. Compared to OI Twake, CTRL Twake based on Tdy has a lower correlation (0.58 versus 0.75) but also a lower absolute mean bias (0.2 versus 0.27) compared to MW Twake. Given the large sample size ($\sim 3 \times 10^4$), and uncertainties associated with satellite-derived SST, TC intensity, translation speed, size, and pre-TC ocean conditions, CTRL Twake computed using Tdy is reasonably well correlated with observed MW Twake, with an explained variance of about 35%. More details on the comparisons between CTRL and MW Twake for different basins are given in Table S2 of the online supporting document.

To assess the potential contribution of a given forcing factor to the coastal–offshore Twake difference, we conduct a suite of sensitivity analyses in which the forcing under consideration is allowed to vary and the other forcings in Tdy are set to constant values. For example, to test the impacts of Vmax on the coastal–offshore Twake difference, we compute Tdy with actual Vmax and other variables in the Tdy formula either set to their global means for global-scale analyses or basin means when analyzing individual basins. The resulting coastal–offshore Twake difference can therefore be attributed to the coastal–offshore variability of Vmax. Similarly, we conduct five separate analyses in which Vtrans, TC size, Grad-T, Grad-S, or MLD are allowed to vary one at a time while the other forcings are set to constants. Note that, in this study, only TCs of at least tropical storm strength are considered (Vmax > 17 m s^{-1}).

3. Results

a. *Twake means: Coastal versus offshore*

Previous studies have discovered that the magnitude of Twake is positively proportional to TC intensity, TC size, and

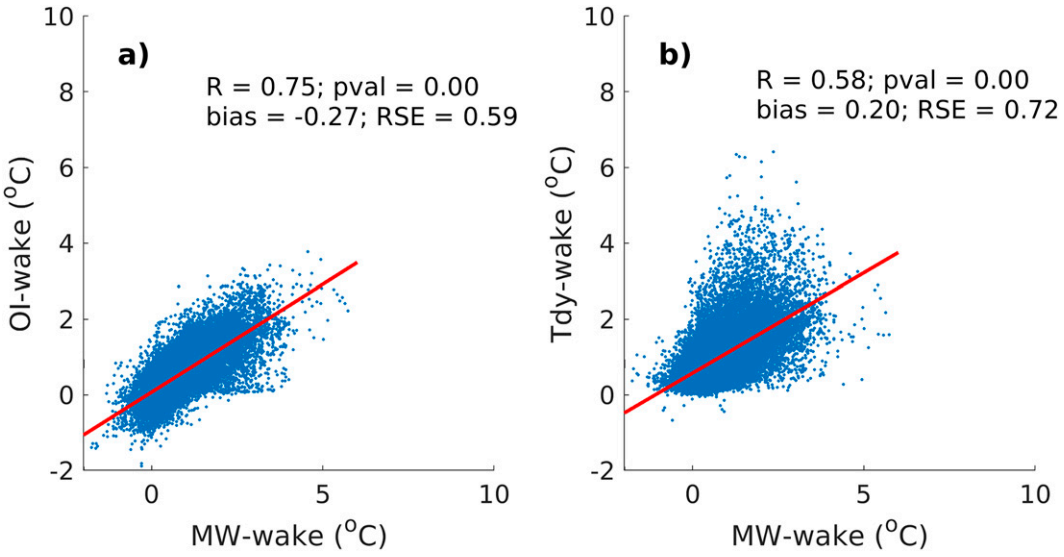

FIG. 4. Relationship between Twakes computed from (a) MW SST and OI SST and (b) MW SST and Tdy CTRL analysis.

temperature stratification, and negatively proportional to TC translation speed, salinity stratification, and mixed layer depth (Price 1981; Cione and Uhlhorn 2003; Vincent et al. 2012). Figure 5 shows maps of correlations between Twake and different forcings. Generally, it confirms the relationships found by previous studies and also reveals the consistency of the relationships in space. Most forcings show a consistent relationship with Twake in space except that salinity shows a more heterogeneous relationship with Twake, probably due to weaker impacts of continental runoff in offshore regions and stronger modulation of the other forcings. However, in regions such as the Bay of Bengal a dominant negative relationship between Twake and salinity stratification is still observed.

Figure 6 compares the mean Twake to the associated forcings in coastal and offshore regions over the 2002–20 period. Coastal Twake is significantly stronger than offshore Twake globally and in all basins except the west Pacific and north Indian (Fig. 6a). The Twake difference is about 0.16°C globally (0.91°C for nearshore compared to 0.75°C offshore) and is largest in the south Indian Ocean, with a difference of 0.32°C, followed by the east Pacific (0.26°C), South Pacific (0.12°C), and North Atlantic (0.06°C) (see Table 1). The coastal–offshore Twake differences also show little sensitivity to bin size variations (see Table S3).

Globally, the difference in TC intensity between coastal and offshore regions is insignificant (Fig. 6b). Yet, looking at individual basins, stronger mean coastal TC intensity supports stronger coastal Twakes in the North Atlantic, south Indian, and South Pacific. In contrast, in the east Pacific, coastal–offshore TC intensity differences oppose the Twake differences.

Similar to intensity, TC translation speed has a mixed contribution to the Twake difference in different basins (Fig. 6c). TC translation speed is lower in coastal regions and contributes to the stronger coastal Twake in the North Atlantic, east Pacific, south Indian, South Pacific, and at global scale. In the northwest Pacific and north Indian basins, TC translation speed in the coastal region is larger than in the offshore region, which tends to support weaker coastal Twake.

Globally, mean TC size (R34) is insignificantly different between coastal and offshore regions (Fig. 6d). Yet, in the basins where coastal Twake is significantly larger than offshore Twake, i.e., the North Atlantic, east Pacific, south Indian, and South Pacific, mean coastal TC size is significantly smaller than offshore TC size. This means that the coastal–offshore TC size differences do not support the Twake differences in those basins.

In the south Indian Ocean, northwest Pacific, and especially east Pacific, pre-TC coastal temperature stratification is significantly larger than offshore temperature stratification, which supports stronger coastal Twakes (Figs. 6a,e). However, there is no difference between coastal and offshore temperature stratification in the North Atlantic and north Indian. In the South Pacific, coastal temperature stratification is weaker than offshore temperature stratification, so it cannot explain the stronger coastal Twake there. Overall, global pre-TC coastal temperature stratification is stronger than offshore temperature stratification mainly due to stronger coastal temperature stratification in the North Pacific basins.

Salinity stratification shows interbasin consistency, with all basins except the south Indian Ocean having stronger coastal than offshore salinity stratification (Fig. 6f). This is likely because continental runoff strongly impacts coastal regions, and it means that salinity stratification cannot be the cause of the stronger coastal Twake in most basins (Figs. 6a,f). The exceptionally weaker salinity stratification in the south Indian Ocean is likely due to a lack of large river systems that discharge into the coastal regions of that basin, and the ITCZ strongly influences salinity stratification in the offshore region (Mamalakis and Foufoula-Georgiou 2018).

In contrast to salinity stratification, MLD is consistently conducive to the coastal–offshore Twake differences in the North

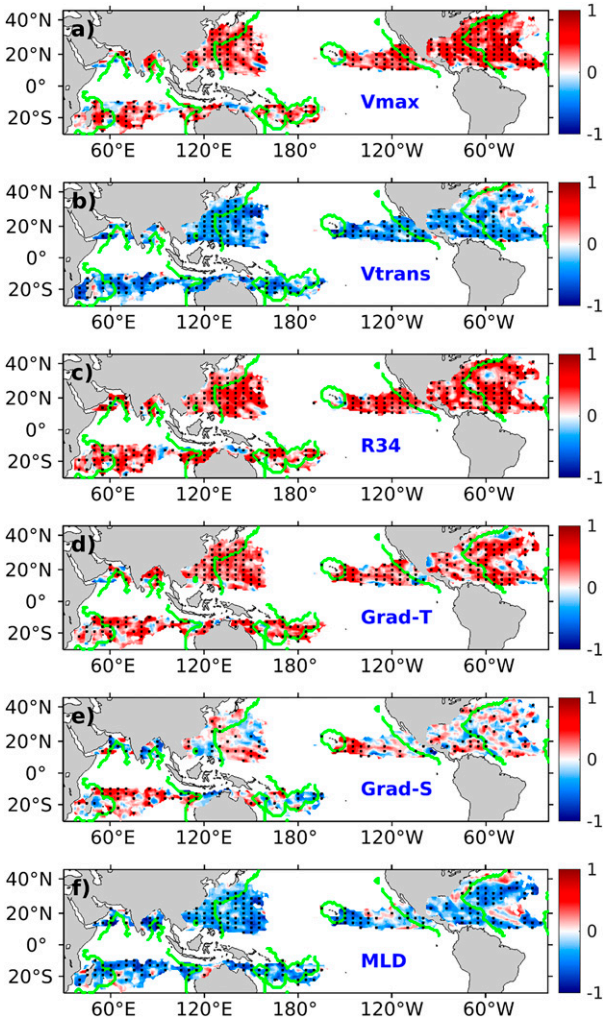

FIG. 5. Maps of correlation between MW Twake and different forcings computed over the period 2002–20. Correlation is computed over a longitude–latitude bin of 5° × 3°. Only bins with more than 20 data points are considered. Locations with correlations that are significant at the 95% level are marked with black dots.

Atlantic, east Pacific, south Indian, and at the global scale. In the two basins with insignificant coastal–offshore Twake differences, the effect of a thinner mixed layer on Twake in coastal regions may be countered by other factors: stronger Grad-S, weaker Vmax, and faster Vtrans in the northwest Pacific, and stronger Grad-S and faster Vtrans in the north Indian Ocean. The reasons for a thinner mixed layer in coastal regions for most basins may be stronger salinity stratification (Fig. 6f), the absorption of solar radiation within shallower depths due to enhanced suspended matter and turbidity, and weaker wind stress due to the close proximity to land (Fig. S4).

In summary, coastal Twakes are significantly stronger than offshore Twakes when averaged globally and also in most individual basins. This is supported by slower TC translation, stronger temperature stratification, and thinner mixed layer in the global coastal ocean, but there is considerable spread when individual basins are considered. Besides the consistent contribution of MLD to the positive coastal–offshore Twake differences in most basins, TC intensity and translation speed contribute to the stronger coastal Twake in the North Atlantic, south Indian, and South Pacific, and temperature stratification contributes to the stronger coastal Twake in the east Pacific. The south Indian Ocean is the only basin in which salinity stratification is conducive to the coastal–offshore Twake difference, whereas in other basins salinity stratification tends to reduce the difference between coastal and offshore Twake. In the northwest Pacific and the north Indian Ocean, contrasting effects of forcings' may cancel each other and result in insignificant differences in Twake between coastal and offshore regions.

b. *The role of different forcings*

The stronger coastal Twake globally implies a greater negative feedback on TC intensity in coastal regions. As shown in the previous section, both TC characteristics and pre-TC ocean conditions contribute to the Twake differences between coastal and offshore regions. Next, we assess quantitatively the relative impacts of pre-TC ocean conditions and TC state on the coastal–offshore Twake differences using the approach outlined in section 2d.

1) RESULTS FROM SUBSAMPLING

Figure 7 shows the subsampled means of Twake and associated forcings. After subsampling, Vmax, Vtrans, and R34 in individual basins and globally have similar mean values (Fig. S5). The subsampled mean Twakes in coastal regions remain stronger than offshore regions globally (Fig. 7a, Table 1), with values of 0.88° and 0.80°C for coastal and offshore regions, respectively. The subsampled coastal–offshore Twake difference of 0.08°C globally is significant, implying an important contribution of ocean pre-TC conditions (MLD and Grad-T) of about 50% to the overall difference of 0.16°C in the full analysis. However, the reduction in Twake difference when subsampling also means that the contribution from TC characteristics (i.e., Vtrans) is important.

Coastal mean subsampled Twake remains stronger than offshore Twake in the east Pacific and south Indian basins. The subsampled coastal–offshore Twake differences in these basins are similar to those from the full analysis: 0.27° versus 0.26°C for the east Pacific and 0.27° versus 0.32°C for the south Indian. These results highlight the importance of ocean pre-TC conditions for the coastal–offshore Twake differences. However, in the North Atlantic and South Pacific, the positive Twake differences become insignificant when subsampling, implying a crucial role for TC characteristics in generating stronger coastal Twakes. In the northwest Pacific and north Indian Ocean, the subsampled coastal–offshore Twake differences remain insignificant, implying that neither coastal–offshore differences in pre-TC ocean conditions nor TC characteristics are strong enough to force coastal–offshore differences in Twakes, or that there are competing influences from different factors.

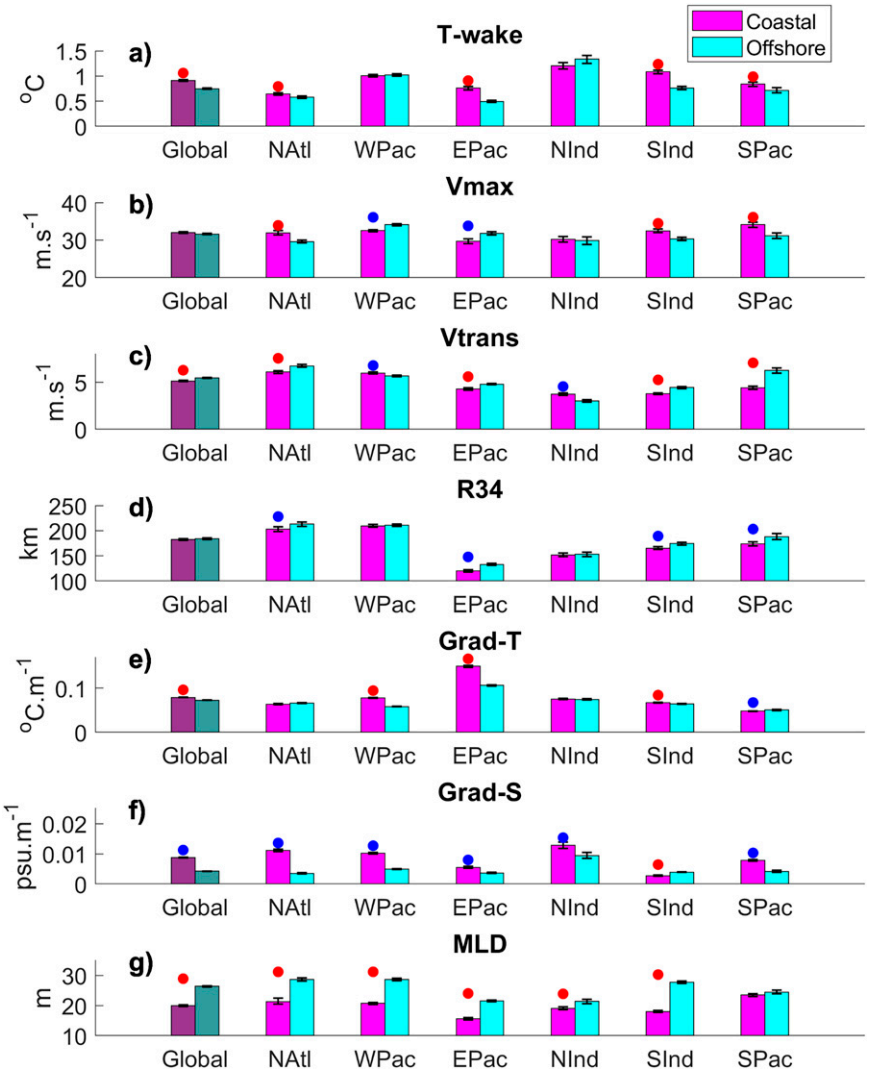

FIG. 6. Mean (a) Twake, (b) TC intensity, (c) translation speed, (d) TC size, (e) temperature stratification, (f) salinity stratification, and (g) mixed layer depth at TC locations in coastal and offshore regions. The means are computed over the 2002–20 period. The circle markers indicate significant differences at the 95% level between coastal and offshore values. The marker colors in (a) represent significantly stronger (red) or weaker (blue) coastal Twake compared to offshore Twake. The maker colors in (b)–(f) are coded so that if the difference of the variable supports the Twake difference in (a), it has the same color as the marker of Twake difference in (a).

In summary, using the subsampling method, we found that TC characteristics and ocean pre-TC conditions are equally important for explaining the global coastal–offshore Twake difference. While TC characteristics (Vmax, Vtrans) dominate the positive coastal–offshore Twake difference in the North Atlantic and the South Pacific, pre-TC ocean conditions dominate the positive coastal–offshore Twake differences in the east Pacific (Grad-T, MLD) and south Indian Ocean (Grad-T, Grad-S, MLD). In the other two basins (northwest Pacific and north Indian), neither TC characteristics nor pre-TC ocean conditions are strong enough to cause a significant difference between coastal and offshore Twakes, or there are competing/canceling effects.

2) RESULTS FROM SENSITIVITY ANALYSES

The subsampling method used in section 3b(1) helps assess the relative importance of two groups of forcings (TC characteristics and ocean pre-TC conditions) to the coastal–offshore Twake differences. In this section, we use the Tdy framework to further assess the roles of individual forcings in driving the coastal–offshore Twake differences. Figure 8 and Table 2 show the coastal–offshore mean Twake differences in the CTRL and sensitivity analyses using all data available. CTRL reproduces well the observed magnitude and significance of coastal–offshore Twake difference at the global scale (0.11° in CTRL versus 0.16°C observed; Table 2) and in most basins

TABLE 1. Coastal and offshore mean Twake in different basins for original data and subsampled data computed using MW SST, and mean Twake computed using the Tdy framework, over the 2002–20 period. Values in bold are significant at the 95% level. NAtl = North Atlantic Ocean; WPac = west Pacific Ocean; EPac = east Pacific Ocean; NInd = north Indian Ocean; SInd = south Indian Ocean; SPac = South Pacific Ocean.

		Global	NAtl	WPac	EPac	NInd	SInd	SPac
Original MW wake (°C)	1. Coastal Twake	0.91	0.64	1.01	0.76	1.21	1.09	0.84
	2. Offshore Twake	0.75	0.58	1.02	0.50	1.34	0.76	0.71
	3. Difference (1 − 2)	**0.16**	**0.06**	−0.02	**0.26**	−0.13	**0.32**	**0.12**
Subsampled MW wake (°C)	4. Coastal Twake	0.88	0.57	1.01	0.75	1.21	1.05	0.76
	5. Offshore Twake	0.80	0.58	1.00	0.49	1.31	0.78	0.83
	6. Difference (4 − 5)	**0.08**	−0.01	0.01	**0.27**	−0.10	**0.27**	−0.06

including the North Atlantic (0.07° versus 0.06°C), east Pacific (0.29° versus 0.26°C), south Indian (0.28° versus 0.32°C), and South Pacific (0.13° versus 0.12°C). CTRL also reproduces well the insignificant Twake difference in the north Indian Ocean. Only in the northwest Pacific does CTRL fail to reproduce the magnitude and significance of the coastal–offshore Twake difference: while MW Twake shows an insignificant value of −0.02°C, CTRL gives a significantly stronger coastal Twake of 0.10°C. Hence there is high confidence in the sensitivity analyses presented below for the global scale and most individual basins.

At the global scale, most forcings result in a significant positive coastal–offshore Twake difference except TC size, which is insignificant, and Grad-S, which is negative (Fig. 8, Table 2). The largest positive contributions to the coastal–offshore Twake difference are from MLD (0.07°C), Vtrans (0.06°C), and Grad-T (0.05°C), and the largest negative influence is from Grad-S (−0.05°C). Combining the forcings into a TC group (Vmax, Vtrans, TC size) and an ocean group (Grad-T, Grad-S, MLD), we can see that, at a global scale, the contributions from TC characteristics and ocean conditions are similar, with total values of 0.08° and 0.07°C, respectively. These results are similar to

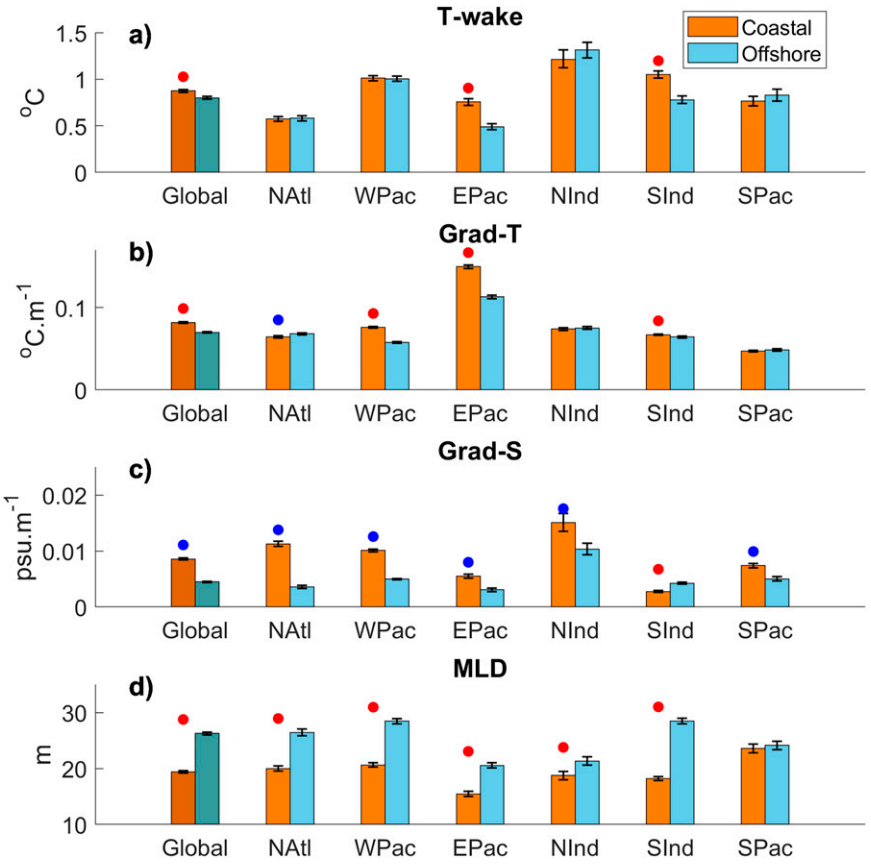

FIG. 7. As in Fig. 6, but for subsampled data. Vmax, Vtrans, R34, and associated Twake, Grad-T, Grad-S are subsampled so that Vmax, Vtrans, and R34 have the same distributions and mean values in coastal and offshore regions.

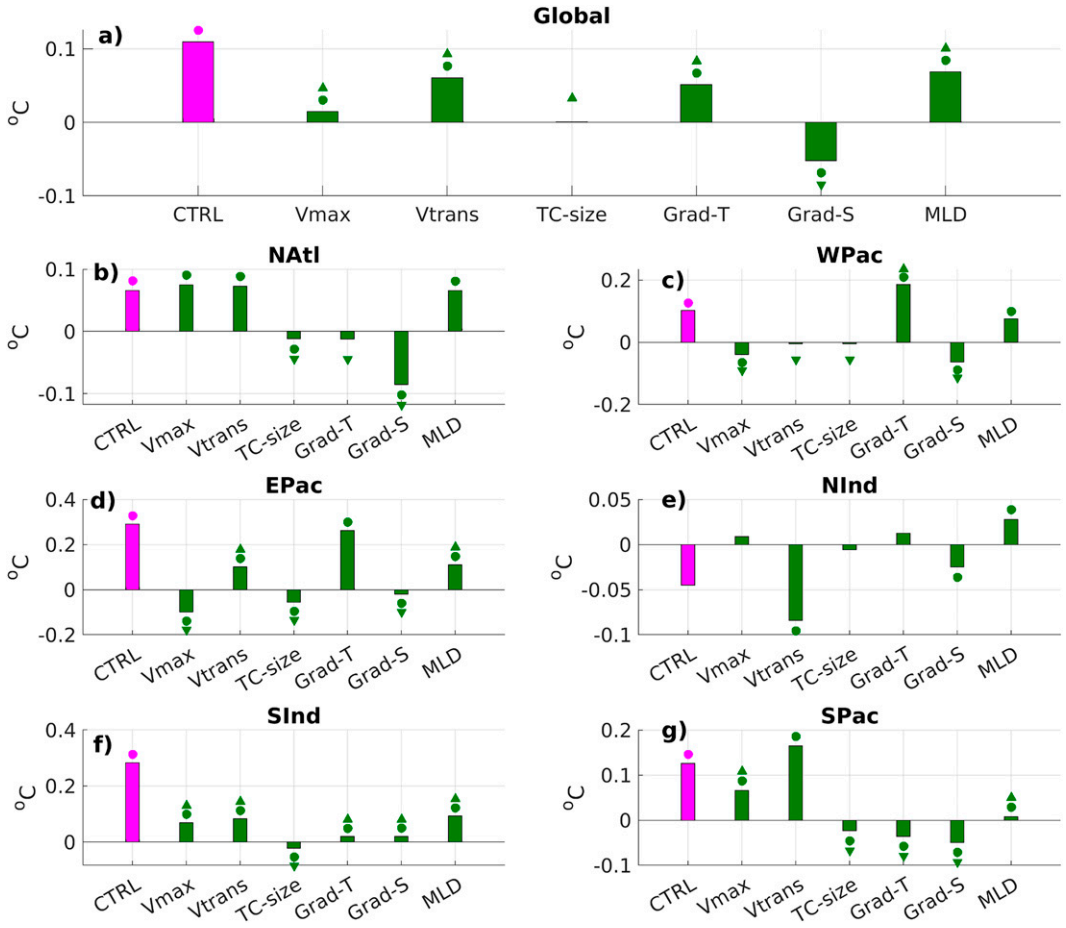

FIG. 8. Difference between coastal and offshore Twake in different sensitivity tests. CTRL is the reference test, and MLD, Grad-T, Grad-S, Vtrans, Vmax, and TC size are tests that use constant MLD, constant Grad-T, constant Grad-S, constant Vtrans, constant Vmax, and constant TC size, respectively. The circle markers represent significant coastal–offshore Twake difference compared to zero (at 95% level). Triangle markers indicate higher and lower values (significant at 95% level) compared to CTRL in the sensitivity tests.

those from the subsampling method which showed that removing the effect of TC characteristics led to about a 50% decrease in the subsampled Twake difference, from 0.16° to 0.08°C.

TC intensity and translation speed were found to dominate the Twake difference in the North Atlantic and the South Pacific using composite analysis (Table 1, Fig. 6) and the subsampling method (Fig. 7). Figures 8b and 8g show the results of the sensitivity tests in these basins. In the North Atlantic, the contribution of Vmax (0.08°C) or Vtrans (0.07°C) alone can reach the level of the Twake difference seen in CTRL

TABLE 2. Coastal–offshore Twake differences (°C) from observations and sensitivity tests in different regions. Values from CTRL test are taken as reference. Bold values are larger or equal to the reference value in absolute magnitude. Italic values represent nonsignificant Twake differences (not different from 0) at the 95% level. Columns 8 and 9 represent the additive effect of TC characteristics (2–4) and ocean conditions (5–7), respectively.

	Obs (0)	CTRL (1)	Vmax (2)	Vtrans (3)	TC size (4)	Grad-T (5)	Grad-S (6)	MLD (7)	TC (8)	Ocean (9)
Global	0.16	0.11	0.01	0.06	*0.00*	0.05	−0.05	0.07	0.08	0.07
NAtl	0.06	0.07	**0.08**	**0.07**	−0.01	*−0.01*	−0.09	**0.07**	**0.14**	−0.03
WPac	*−0.02*	0.10	−0.04	*0.00*	*0.00*	**0.19**	−0.06	0.08	−0.05	**0.20**
EPac	0.26	0.29	−0.10	0.10	−0.06	0.26	−0.02	0.11	−0.05	**0.35**
NInd	*−0.13*	*−0.04*	0.01	−0.08	*−0.01*	*0.01*	−0.02	0.03	−0.08	0.02
SInd	**0.32**	0.28	0.07	0.08	−0.02	0.02	0.02	0.09	0.13	0.13
SPac	0.12	0.13	0.07	**0.16**	−0.02	−0.04	−0.05	0.01	**0.21**	−0.08

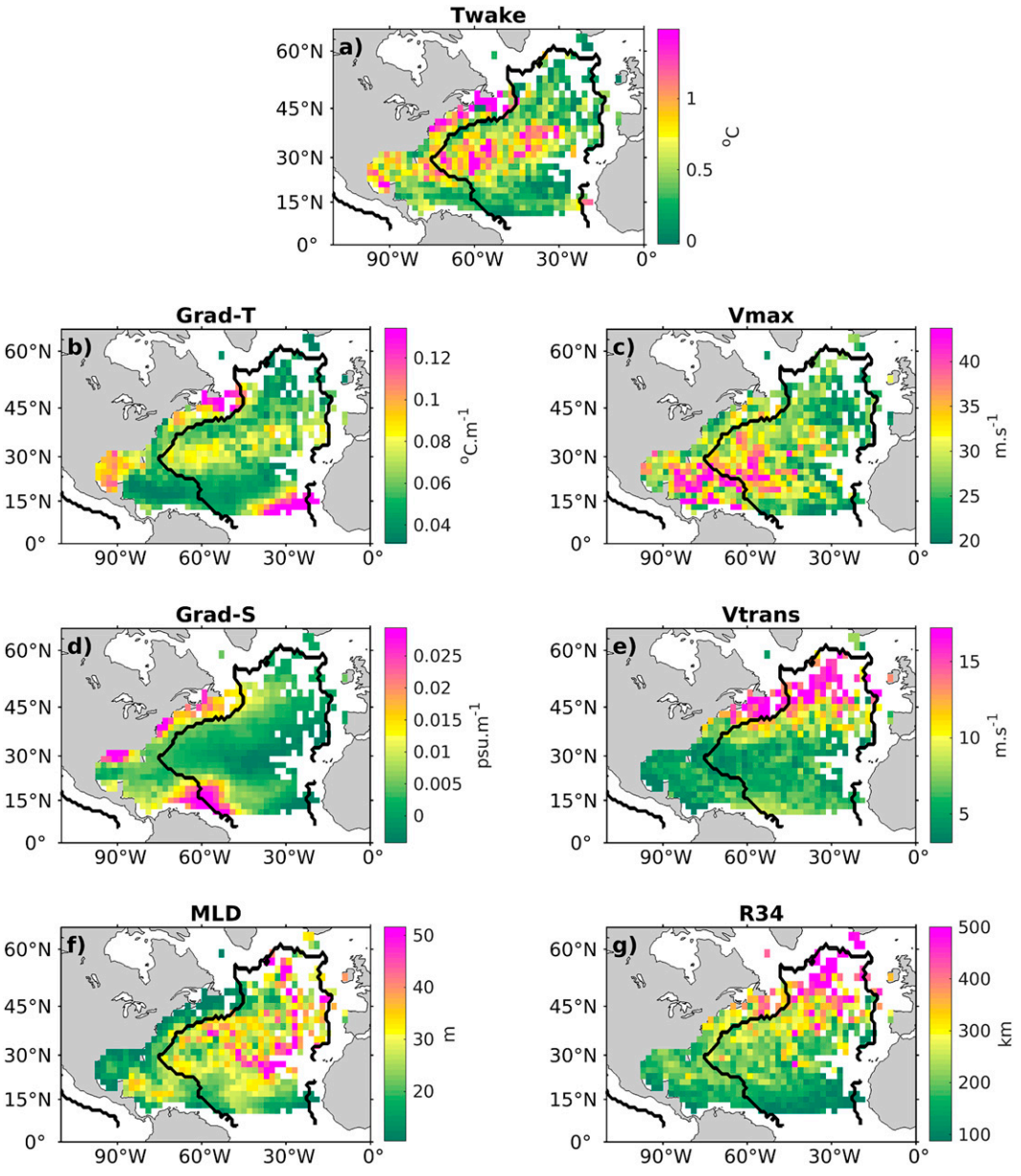

FIG. 9. North Atlantic mean maps of (a) TC induced ocean cooling, (b) pre-TC ocean temperature stratification, (c) TC intensity, (d) pre-TC salinity stratification, (e) TC translation speed, (f) pre-TC mixed layer depth, and (g) TC size. The values are computed over the period 2002–20 using a longitude–latitude bin of 4° × 4° and all available data with Vmax > 17 m s^{-1}. Only bins with at least three data points are plotted. The black contours separate coastal and offshore regions.

(0.07°C) (see Table 2). Grad-S and MLD largely oppose, confirming the results from the subsampling technique (Figs. 6f,g and 7c,d). In the South Pacific, Vtrans alone can result in a larger Twake difference (0.16°C) than in CTRL (0.12°C), highlighting its dominant role in driving the Twake difference. Vmax also contributes significantly to the positive Twake difference in CTRL with a value of 0.07°C. The sensitivity tests, therefore, confirm the dominant role of TC intensity and translation speed in generating the positive Twake differences in the North Atlantic and South Pacific, consistent with the subsampling method.

From the subsampling results [section 3b(1)], ocean conditions were found to be more important than TC characteristics for the Twake differences in the east Pacific and south Indian Ocean. The sensitivity tests give consistent results in the east Pacific, but not in the south Indian (Figs. 8d,f). In the east Pacific, Grad-T alone gives a Twake difference that is similar to that in CTRL (Fig. 8d). The effect of Grad-T is more than twice as large as the next two factors combined (MLD, 0.11°C; Vtrans, 0.10°C). Here, strong coastal upwelling and related processes are likely responsible for a shallow thermocline and a large Grad-T.

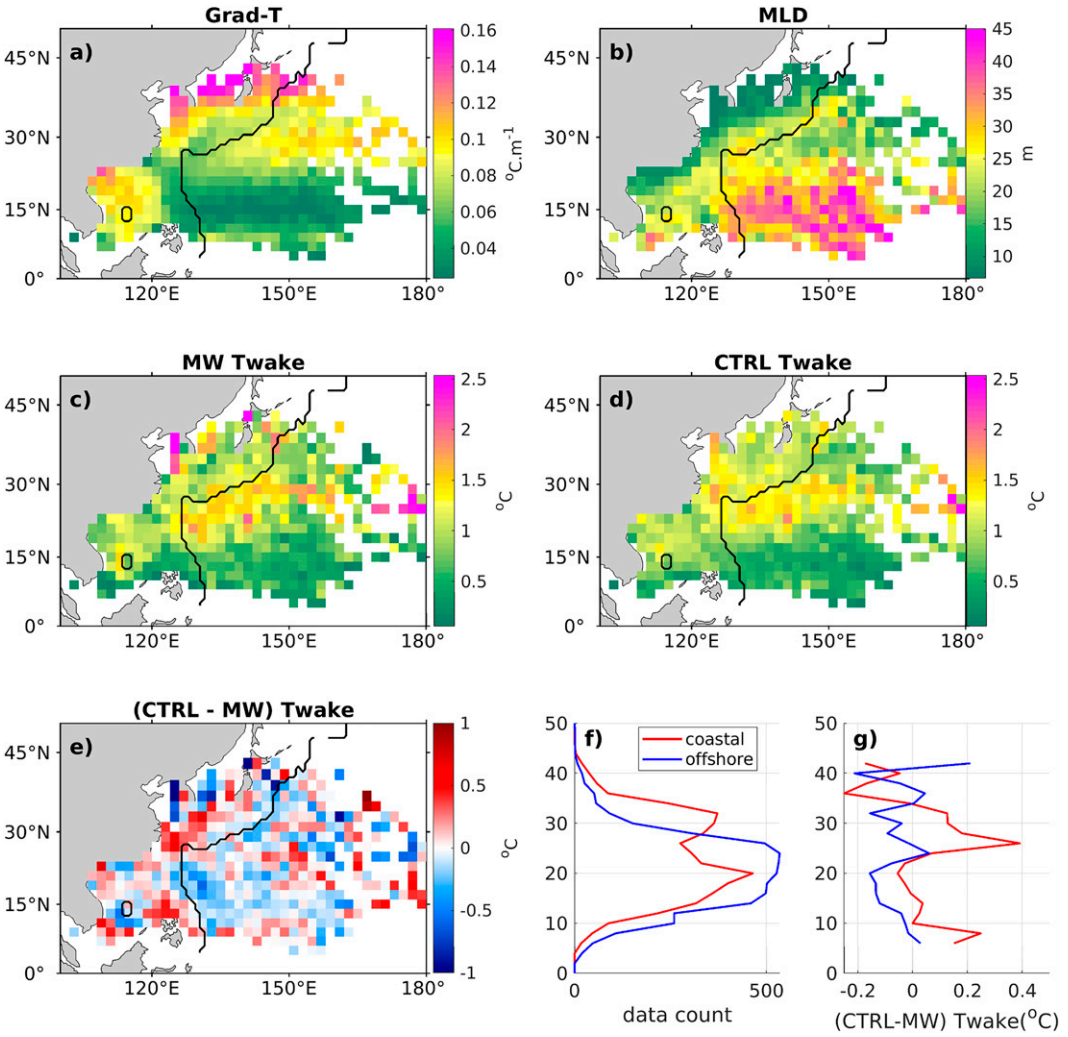

FIG. 10. Comparison between CTRL and observed Twake over the northwest Pacific: mean maps of (a) pre-TC temperature stratification and (b) MLD, (c) MW Twake, (d) CTRL Twake, (e) difference between CTRL and MW Twake, (f) meridional distribution of data in coastal and offshore regions, and (g) meridional mean of difference of Twake between CTRL and MW over coastal and offshore regions.

In the south Indian Ocean, however, both Vmax and Vtrans result in significant positive Twake differences of 0.07° and 0.08°C, respectively. The sum of the TC forcings and the sum of the ocean forcings are equal (0.13°C), meaning that the two groups are equally important to the Twake difference in the south Indian Ocean, which is contrary to the results using the subsampling method. These contrasting results will be investigated further in section 3c(e).

In the northwest Pacific and north Indian, both the original and subsampled Twake differences were found to be insignificant (Figs. 6a and 7a). In the north Indian Ocean, CTRL also produces an insignificant Twake difference (Fig. 8e, Table 2), possibly due to the low TC sample size. In the northwest Pacific, the effects of Vtrans and TC size are insignificant, whereas the effect of Vmax is significantly negative (−0.04°C). Therefore, the positive Twake difference in the northwestern Pacific is mainly driven by ocean forcings. Of the three ocean forcings, Grad-T results in a Twake difference of 0.19°C, which dominates the contributions of MLD (0.08°C) and Grad-S (−0.06°C).

c. *The uniqueness of different basins*

The results in sections 3a and 3b reveal strong interbasin variability of the coastal–offshore Twake difference and its relationships with different forcings. Here we investigate distinct features in certain basins.

1) THE NORTH ATLANTIC: ROLE OF TEMPERATURE STRATIFICATION

The subsampling and sensitivity analyses reveal the dominant roles of Vmax and Vtrans for the overall coastal–offshore Twake difference in the North Atlantic. However, there is strong intrabasin variability. There is little difference between coastal and

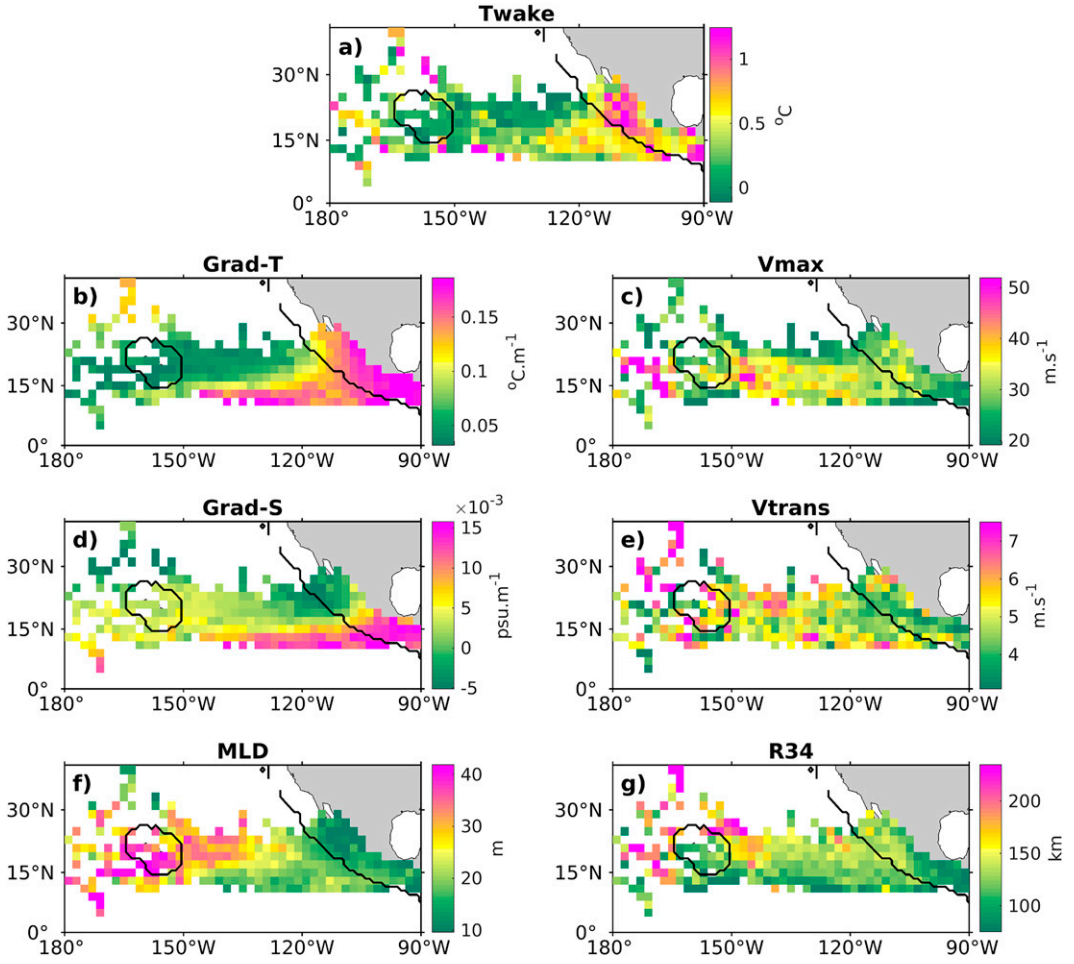

FIG. 11. East Pacific means maps of Twake and forcings (similar to Fig. 9).

offshore Twakes at low latitudes (south of 35°N) but a large difference north of 35°N (Fig. 9a). Only MLD and temperature stratification have strong coastal–offshore differences that support the Twake differences north of 35°N. This means that over higher latitudes, the coastal–offshore Twake difference is mainly driven by MLD and temperature stratification. However, Glenn et al. (2016) revealed that baroclinic processes contribute to strong coastal Twakes in the Mid-Atlantic Bight, highlighting the importance of other phenomena in the nearshore regions in addition to TC characteristics and ocean mixing processes.

Of the forcings, the spatial variability of Grad-T best agrees with Twake (Fig. 9). The spatial correlation computed from the mean maps is also highest between Twake and Grad-T (0.46), followed by MLD (0.34) and Vmax (0.32), all significant at the 95% level. An important question is why the crucial role of Grad-T in the North Atlantic is not reflected in the overall statistics in Fig. 6d and the results of the sensitivity test in Fig. 8b. The 0°–18°N band, where coastal Grad-T is much lower than offshore Grad-T, is the main cause of the larger basin-averaged offshore Grad-T compared to near-coastal (Fig. S6). In this latitude band, there is a region of extremely high Grad-T off the African coast that is associated with only weak Vmax and moderate Twake (Fig. 9b). Excluding the 0°–15°N band from the computations of the means of Twake and Grad-T results in the expected relationship between Twake and Grad-T (stronger Grad-T associated with larger Twake) over a large range of latitudes between 18° and 57°N (Fig. S6). Also, this highlights the complexity of the signal due to differences in spatial variability of forcings.

2) THE NORTHWEST PACIFIC: UNCERTAIN ROLE OF TEMPERATURE STRATIFICATION

The northwest Pacific is the basin with the largest discrepancy between the observed and Tdy-predicted Twake from the sensitivity tests (CTRL; Table 2). Whereas Tdy predicts a stronger mean coastal Twake due to significantly thinner mixed layer and stronger Grad-T, observed Twake does not show any coastal–offshore difference. To investigate the reasons behind the discrepancy, we show in Figs. 10a and 10b the mean maps of Grad-T and MLD. Grad-T is stronger and MLD is thinner in the near-coastal region at most latitudes. The Tdy CTRL reproduces well the spatial patterns of observed Twake in the northwest Pacific (Figs. 10c,d). However, Figs. 10f and 10g reveal that the regions of strongest

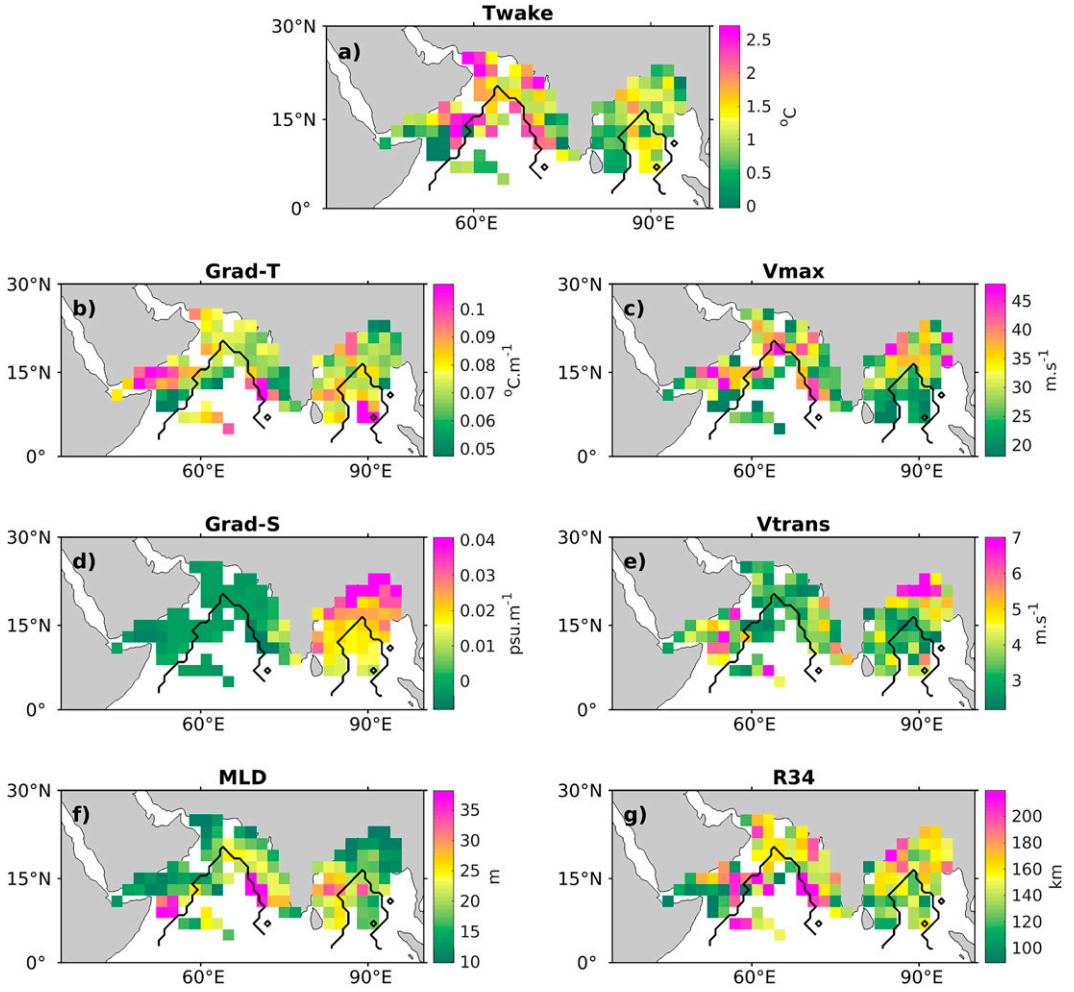

FIG. 12. North Indian Ocean means maps of Twake, and forcings (similar to Fig. 9).

disagreement between the CTRL and observed Twake are generally in the 26°–32°N latitude band, where there is a southwest to northeast oriented track of larger CTRL Twakes compared to observed Twakes (i.e., positive bias in Fig. 10e). The bias does not appear to be due to a simple lack of data because the data count is fairly steady at those latitudes (Fig. 10f).

When we use a gridded observational dataset (EN4) instead of SODA the bias between CTRL and observed Twake is similar. This suggests that the combination of strong horizontal gradients in Grad-T and uneven spatial and/or temporal ocean sampling in that region may result in an overestimation of near-coastal Twake in CTRL. Further studies are required to assess further the representativeness of temperature stratification in the near-coastal region and its importance for the coastal–offshore Twake difference.

3) THE EAST PACIFIC: DOMINANT ROLE OF TEMPERATURE STRATIFICATION

Previously we found that ocean temperature stratification is particularly important for the coastal–offshore Twake difference in the east Pacific basin. Figure 11 shows a distinct maximum in Twake with a triangle shape in the near-coastal region west of Mexico that coincides with strong Grad-T and thin mixed layer, confirming the important role of ocean stratification (Grad-T and MLD) for the coastal–offshore Twake difference. In contrast, in the maps of other forcings, the patterns found in Twake are less coherent. The spatial correlations of Grad-T and MLD with Twake are also larger in magnitude than those with other forcings. The correlations for Twake with Grad-T and MLD are 0.58 and −0.49, respectively, followed by Vtrans (−0.42), Vmax (0.19), and Grad-S (0.19).

4) THE NORTH INDIAN OCEAN: IMPORTANCE OF SALINITY STRATIFICATION

Figure 12 shows the spatial distributions of the means of Twake and related forcings over the north Indian Ocean. There is considerable asymmetry in the coastal and offshore areas due to the presence of the Indian Peninsula, which extends southward to almost 5°N and divides the ocean into two parts: the Bay of Bengal and the Arabian Sea. The north Indian Ocean is

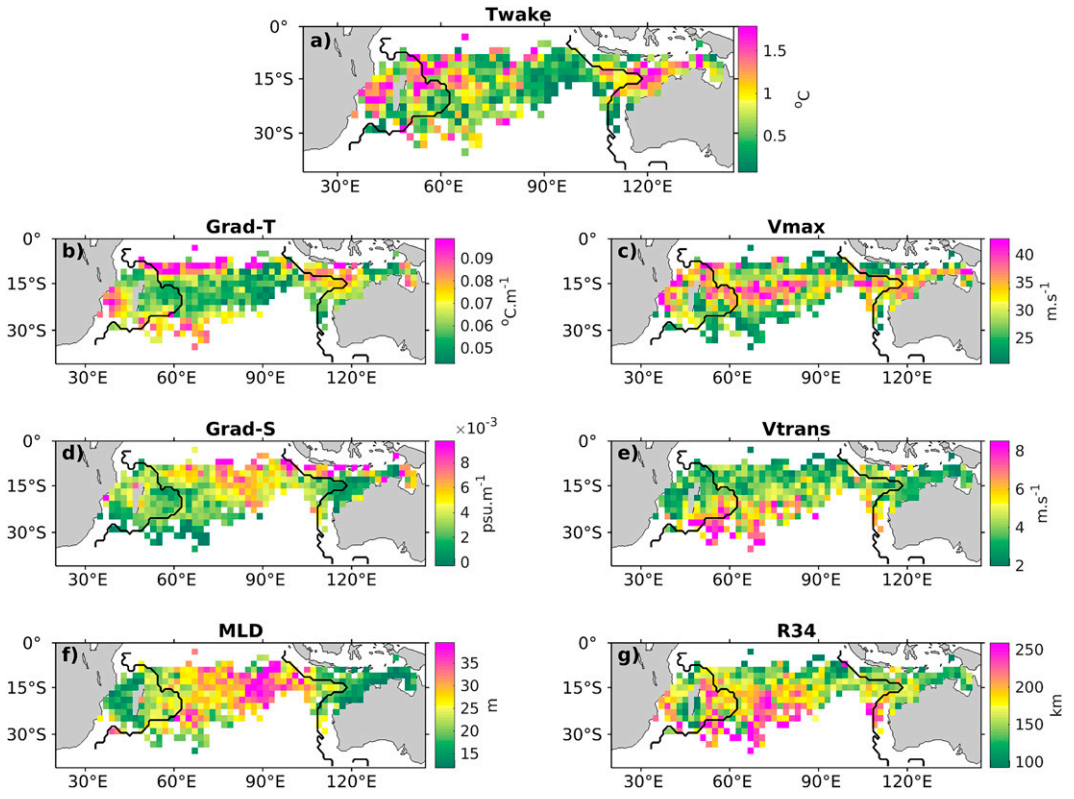

FIG. 13. South Indian Ocean mean maps of Twake and forcings (similar to Fig. 9).

also the only basin with more coastal data than offshore data (larger by a factor of 2; Table S1). Salinity stratification is much stronger in coastal regions in the Bay of Bengal, whereas there is not much difference in the Arabian Sea. This is due to strong postmonsoon river runoff in the Bay of Bengal, which forms a thin layer of freshwater that prevents wind-induced mixing and maintains a deep warm layer, resulting in a weak Twake (Sengupta et al. 2008). Because there are more TCs in the Bay of Bengal, it dominates the mean signal and results in overall weaker coastal Twake in the north Indian Ocean.

5) THE SOUTH INDIAN OCEAN: COMBINED TC AND OCEAN FORCING

Among the six basins, the south Indian Ocean is associated with the strongest observed coastal–offshore Twake difference of 0.28°C. While the subsampling method revealed a stronger role of ocean forcing, the sensitivity tests showed similar contributions from the ocean state and TC characteristics. The reasons for the apparent discrepancy are the unique spatial distributions of ocean and TC forcing factors in the south Indian Ocean (Fig. 13) and the fact that our linear methods (subsampling and Tdy sensitivity analysis) do not fully account for them. Near both the eastern and western boundaries of the basin, there are regions with stronger Grad-T and Vmax, weaker Grad-S, slower Vtrans, and thinner MLD compared to the offshore region. This means that 5 out of 6 forcings (except R34) are acting to generate stronger coastal Twakes. Another main reason for the large coastal–offshore Twake difference is the presence of a minimum Twake zone in the offshore region east of 80°E. This area is associated with weak Grad-T, strong Grad-S, thick mixed layer, small TC size, and weaker than average Vmax. Comparing the spatial patterns of TC characteristics and ocean forcings, we can see that all TC forcings show more meridional variation, whereas salinity stratification and MLD show stronger zonal variations that agree better with the Twake spatial distribution. The overall spatial correlations computed using the mean maps also confirm the strong influence of Grad-T over Twake (correlation of 0.50), followed by MLD (−0.42), Vtrans (−0.21), and Vmax (0.17). This suggests a larger role for ocean forcings in the coastal–offshore Twake difference of the south Indian Ocean, consistent with the subsampling method shown previously.

4. Conclusions and discussion

In summary, using satellite SST observations over the 2002–20 period, we found stronger mean Twakes in coastal regions compared to the open ocean at the global scale and in all basins except the northwest Pacific and north Indian Ocean. We found that stronger coastal Twakes are driven mainly by higher mean TC intensity and lower translation speed in the South Pacific, by stronger temperature stratification in the North Atlantic and the east Pacific, and by all ocean forcings in the south Indian Ocean.

In the northwest Pacific and north Indian Ocean, forcings tend to counter each other, resulting in similar coastal and offshore mean Twakes.

In some basins there are strong regional differences in the coastal–offshore Twake contrast and its regulation by ocean stratification and mixed layer depth. In the North Atlantic, the strongest positive coastal–offshore Twake difference is observed over the Mid-Atlantic Bight, driven by very strong coastal–offshore contrasts of temperature stratification and MLD. In the north Indian Ocean, the strongest coastal–offshore Twake difference is in the Bay of Bengal, where salinity stratification plays a dominant role. In the south Indian Ocean, the strongest coastal–offshore Twake difference is located in the eastern part of the basin where there is a pronounced thinning of the mixed layer, strengthening of temperature stratification, and weakening of salinity stratification toward the coast. These findings suggest that models need to simulate the observed near-coastal/offshore difference in ocean stratification and SST cooling properly. If the contrast is too weak in models, they may predict TCs that are too strong near the coast and/or too weak offshore. The uniqueness of the Indian Ocean further emphasizes the importance of subsurface salinity observations there. In addition, it is unclear how coastal and offshore ocean stratification and mixed layer depth might change under global warming. Any changes in the coastal–offshore stratification and mixed layer depth contrast will likely impact TC-induced SST cooling and may affect TC intensification near landfall.

Despite the new insights into TC–ocean interactions revealed by the subsampling method and the sensitivity analyses based on the Tdy framework, these methods still have limitations and the results should be interpreted with caution. The importance of temperature stratification in many areas of the North Atlantic, but not for the basin as a whole, is an example of the limitation of explaining the mean Twake using mean forcings. There are also limitations associated with the idealized Tdy framework that was used to isolate the effect of different forcing factors. For example, it does not explicitly account for SST cooling from the surface heat flux or upwelling, which can be important for weaker storms and larger, slower-moving storms, respectively. We also did not consider the role of ocean depth variations in the near-coastal region. More in-depth analyses with stand-alone ocean and fully coupled models are needed to address these questions.

Acknowledgments. GRF and NDD were supported by base funds to AOML's Physical Oceanography Division. NDD acknowledges support from the Department of Oceanography, Faculty of Hydrology Meteorology and Oceanography, VNU University of Science and ISCALE Computing Solution JSC, Vietnam. KB is supported by the Office of Science (BER) of the U.S. Department of Energy as part of the Regional and Global Model Analysis (RGMA) program area through the Water Cycle and Climate Extremes Modeling project and the collaborative multiprogram Integrated Coastal Modeling project. EF was supported in part by the U.S. Department of Energy, Office of Science, Office of Workforce Development for Teachers and Scientists (WDTS) under the Science Undergraduate Laboratory Internships Program (SULI). The Pacific Northwest National Laboratory is operated for DOE by Battelle Memorial Institute under Contract DE-AC05-76RL01830.

Data availability statement. All data used in this study are available publicly from the following websites: storm-track data: https://www.ncdc.noaa.gov/ibtracs/; OI SST data: https://www.ncdc.noaa.gov/oisst; MW SST data: www.remss.com; SODA data: http://www.soda.umd.edu/.

REFERENCES

Balaguru, K., G. R. Foltz, L. R. Leung, E. D. Asaro, K. A. Emanuel, H. Liu, and S. E. Zedler, 2015: Dynamic potential intensity: An improved representation of the ocean's impact on tropical cyclones. *Geophys. Res. Lett.*, **42**, 6739–6746, https://doi.org/10.1002/2015GL064822.

Bender, M. A., I. Ginis, and Y. Kurihara, 1993: Numerical simulations of tropical cyclone-ocean interaction with a high-resolution coupled model. *J. Geophys. Res.*, **98**, 23 245–23 263, https://doi.org/10.1029/93JD02370.

Cangialosi, J. P., E. Blake, M. DeMaria, A. Penny, A. Latto, E. Rappaport, and V. Tallapragada, 2020: Recent progress in tropical cyclone intensity forecasting at the National Hurricane Center. *Wea. Forecasting*, **35**, 1913–1922, https://doi.org/10.1175/WAF-D-20-0059.1.

Carton, J. A., G. A. Chepurin, and L. Chen, 2018: SODA3: A new ocean climate reanalysis. *J. Climate*, **31**, 6967–6983, https://doi.org/10.1175/JCLI-D-18-0149.1.

Cione, J. J., and E. W. Uhlhorn, 2003: Sea surface temperature variability in hurricanes: Implications with respect to intensity change. *Mon. Wea. Rev.*, **131**, 1783–1796, https://doi.org/10.1175//2562.1.

Da, N. D., G. R. Foltz, and K. Balaguru, 2020: A satellite-derived upper-ocean stratification data set for the tropical North Atlantic with potential applications for hurricane intensity prediction. *J. Geophys. Res. Oceans*, **125**, e2019JC015980, https://doi.org/10.1029/2019JC015980.

——, ——, and ——, 2021: Observed global increases in tropical cyclone-induced ocean cooling and primary production. *Geophys. Res. Lett.*, **48**, e2021GL092574, https://doi.org/10.1029/2021GL092574.

Efron, B., 1992: *Bootstrap Methods: Another Look at the Jackknife*. Springer, 569–593.

Emanuel, K., 2003: Tropical cyclones. *Annu. Rev. Earth Planet. Sci.*, **31**, 75–104, https://doi.org/10.1146/annurev.earth.31.100901.141259.

Glenn, S. M., and Coauthors, 2016: Stratified coastal ocean interactions with tropical cyclones. *Nat. Commun.*, **7**, 10887, https://doi.org/10.1038/ncomms10887.

Gramer, L. J., J. A. Zhang, G. Alaka, A. Hazelton, and S. Gopalakrishnan, 2022: Coastal downwelling intensifies landfalling hurricanes. *Geophys. Res. Lett.*, **49**, e2021GL096630, https://doi.org/10.1029/2021GL096630.

Guan, S., and Coauthors, 2021: Tropical cyclone-induced sea surface cooling over the Yellow Sea and Bohai Sea in the 2019 Pacific typhoon season. *J. Mar. Syst.*, **217**, 103509, https://doi.org/10.1016/j.jmarsys.2021.103509.

Kaplan, J., M. DeMaria, and J. A. Knaff, 2010: A revised tropical cyclone rapid intensification index for the Atlantic and eastern North Pacific basins. *Wea. Forecasting*, **25**, 220–241, https://doi.org/10.1175/2009WAF2222280.1.

Knapp, K. R., H. J. Diamond, J. P. Kossin, M. C. Kruk, and C. J. Schreck, 2018: International Best Track Archive for Climate

Stewardship (IBTrACS) project, version 4. NOAA National Centers for Environmental Information, accessed 7 January 2023, https://doi.org/10.25921/82ty-9e16.

Lin, I.-I., W. T. Liu, C.-C. Wu, J. C. H. Chiang, and C.-H. Sui, 2003: Satellite observations of modulation of surface winds by typhoon-induced upper ocean cooling. *Geophys. Res. Lett.*, **30**, 1131, https://doi.org/10.1029/2002GL015674.

Mahapatra, D. K., A. D. Rao, S. V. Babu, and C. Srinivas, 2007: Influence of coast line on upper ocean's response to the tropical cyclone. *Geophys. Res. Lett.*, **34**, L17603, https://doi.org/10.1029/2007GL030410.

Mamalakis, A., and E. Foufoula-Georgiou, 2018: A multivariate probabilistic framework for tracking the intertropical convergence zone: Analysis of recent climatology and past trends. *Geophys. Res. Lett.*, **45**, 13 080–13 089, https://doi.org/10.1029/2018GL079865.

Pielke, R., J. Gratz, C. Landsea, D. Collins, M. Saunders, and R. Musulin, 2008: Normalized hurricane damage in the United States: 1900–2005. *Nat. Hazards Rev.*, **9**, 29–42, https://doi.org/10.1061/(ASCE)1527-6988(2008)9:1(29).

Price, J. F., 1981: Upper ocean response to a hurricane. *J. Phys. Oceanogr.*, **11**, 153–175, https://doi.org/10.1175/1520-0485(1981)011<0153:UORTAH>2.0.CO;2.

Sengupta, D., B. R. Goddalehundi, and D. S. Anitha, 2008: Cyclone-induced mixing does not cool SST in the post-monsoon north Bay of Bengal. *Atmos. Sci. Lett.*, **9**, 1–6, https://doi.org/10.1002/asl.162.

Seroka, G., T. Miles, Y. Xu, J. Kohut, O. Schofield, and S. Glenn, 2016: Hurricane Irene sensitivity to stratified coastal ocean cooling. *Mon. Wea. Rev.*, **144**, 3507–3530, https://doi.org/10.1175/MWR-D-15-0452.1.

Shen, W., and I. Ginis, 2003: Effects of surface heat flux-induced sea surface temperature changes on tropical cyclone intensity. *Geophys. Res. Lett.*, **30**, 1933, https://doi.org/10.1029/2003GL017878.

Vincent, E. M., M. Lengaigne, J. Vialard, G. Madec, N. C. Jourdain, and S. Masson, 2012: Assessing the oceanic control on the amplitude of sea surface cooling induced by tropical cyclones. *J. Geophys. Res.*, **117**, C05023, https://doi.org/10.1029/2011JC007705.

Wang, S., and R. Toumi, 2021: Recent tropical cyclone changes inferred from ocean surface temperature cold wakes. *Sci. Rep.*, **11**, 22269, https://doi.org/10.1038/s41598-021-01612-9.

Zhang, J., Y. Lin, D. R. Chavas, and W. Mei, 2019: Tropical cyclone cold wake size and its applications to power dissipation and ocean heat uptake estimates. *Geophys. Res. Lett.*, **46**, 10 177–10 185, https://doi.org/10.1029/2019GL083783.

Zhu, T., and D.-L. Zhang, 2006: The impact of the storm-induced SST cooling on hurricane intensity. *Adv. Atmos. Sci.*, **23**, 14–22, https://doi.org/10.1007/s00376-006-0002-9.